Nuclear isotope thermometry

S. R. Souza,[1] W. P. Tan,[2] R. Donangelo,[1] C. K. Gelbke,[2] W. G. Lynch,[2] and M. B. Tsang[2]
[1]*Instituto de Fisica, Universidade Federal do Rio de Janeiro Cidade Universitária, CP 68528, 21945-970 Rio de Janeiro, Brazil*
[2]*Department of Physics and Astronomy and National Superconducting Cyclotron Laboratory, Michigan State University, East Lansing, Michigan 48824*

(Received 4 April 2000; published 10 November 2000)

We discuss different aspects which might influence temperatures deduced from experimental isotopic yields in the multifragmentation process. It is shown that fluctuations due to the finite size of the system and distortions due to the decay of hot primary fragments conspire to blur the temperature determination in multifragmentation reactions. These facts suggest that caloric curves obtained through isotope thermometers, which were taken as evidence for a first-order phase transition in nuclear matter, should be investigated very carefully.

PACS number(s): 24.60.−k, 25.70.Pq, 21.65.+f

I. INTRODUCTION

Due to the short-range attraction between nucleons, nuclear matter is a Fermi liquid [1] at low temperature, and is expected to undergo a phase transition to a nucleonic gas within a mixed-phase region bounded by a critical temperature of order 15 MeV [2,3]. Experimental investigations of this phase transition have focused on a variety of experimental observables ranging from the mass, charge, or multiplicity distributions for the emitted fragments [4,5], to observables sensitive to the temperature of the system [6,7].

Temperature measurements, in particular, have been performed to search for evidence of the enhanced heat capacity predicted by statistical model calculations reflecting the latent heat for transforming the Fermi liquid to the nucleonic vapor [6–8]. For example, the statistical multifragmentation model (SMM) [9] predicts a plateau of roughly constant temperature of $T \approx 5$ MeV for excitation energies of $E^*/A \approx 3-7$ MeV. At these excitation energies the model predicts a mixed phase consisting of fragments (liquid) and nucleons and light particles (gas) corresponding to a mixed-phase equilibrium. This is followed at higher excitation energies by a linear rise in the temperature with excitation energy, as expected for a gas of small nuclei having negligible internal heat capacity [9]. Similar effects are predicted by the microcanonical Metropolis Monte Carlo model [10].

This trend was qualitatively reproduced in some experiments [7], but not in others [11–14]. An essential part of these measurements is the determination of the temperature of the fragmenting system. Temperatures were extracted from the isotopic abundances of helium and lithium fragments, using the isotope thermometry method proposed by Albergo *et al.* [15]. The idea of the method is to determine the double ratios of the yields of four suitably chosen isotopes, (A_1,Z_1), (A_1+1,Z_1), (A_2,Z_2), and (A_2+1,Z_2), and

$$\frac{Y(A_1,Z_1)/Y(A_1+1,Z_1)}{Y(A_2,Z_2)/Y(A_2+1,Z_2)} = C\exp(\Delta B/T_{iso}), \qquad (1)$$

where Y's are the yields of the different isotopes, C is a constant related to spin values and kinematic factors, $\Delta B = B(A_1,Z_1) - B(A_1+1,Z_1) - B(A_2,Z_2) + B(A_2+1,Z_2)$ is obtained from the binding energies of the isotopes appearing in Eq. (1), and T_{iso} stands for the temperature deduced from this isotopic thermometer. In the case of the He-Li thermometer employed in Ref. [7], $A_1=6$, $Z_1=3$, $A_2=3$, and $Z_2=2$. For the C-Li thermometer, more recently considered by Xi *et al.* [14], $A_1=6$, $Z_1=3$, $A_2=11$, and $Z_2=6$. For the Carbon thermometer studied in this work, $A_1=12$, $Z_1=6$, $A_2=11$, and $Z_2=6$.

However, there are a few aspects which should be carefully analyzed when one wants to compare information on the breakup configuration of an excited system formed in a heavy-ion collision to multifragmentation models like the SMM approach. Some of these points are addressed below. In Sec. II we briefly discuss the assumptions underlying this method. Variations in the temperature of the breakup stage, where the hot primary fragments decouple from the system, are intrinsic to finite systems and are explored within the SMM approach in Sec. III. An analytical description of temperature variations is developed in the grand canonical limit in Sec. IV; this description is consistent with the results from the SMM. In addition, there are finite-size effects, discussed in Sec. V, that make the concept of an overall chemical potential somewhat inaccurate. The influence of secondary decay is discussed in Sec. VI. Conclusions are drawn in Sec. VII.

II. UNDERLYING ASSUMPTIONS

The basic physical hypotheses of the isotope thermometry method are as follows.

(1) An equilibrated source is formed after the most violent stages of the reaction and it decays simultaneously and statistically.

(2) For the experimental event selection employed in the analyses, all the events correspond to fragments formed at the same temperature.

(3) Distortions on the isotopic temperature due to secondary decay of hot primary fragments may be neglected.

Although the statistical multifragmentation model [9], used in the discussion below, is based on the first assumption; the last two hypotheses are not supported by the model, as we shall discuss in detail.

The SMM uses the Monte Carlo method and averages observables with the statistical weight over decay partitions. A multifragment decay partition is *defined* in the SMM approach [9] as a specific set of emitted fragments and light particles. For simplicity, each partition in the SMM approach is weighted according to the entropy of the partition. This entropy is approximated by analytical expressions rather than by an event by event sampling of the phase space as in Ref. [10]. These approximations rely upon that fact that the dominant contribution to this entropy comes from the internal phase space of fragments which plays the role of a heat bath within the SMM approach, just as an excited residue plays the role of a heat bath within compound nuclear decay theory [16].

For a given decay partition and by making a Wigner-Seitz approximation to the Coulomb energy, energy conservation within the SMM approach leads to the expression [9]

$$E_0^{\text{g.s.}}+E_0^*=\frac{3}{5}\frac{Z_0^2e^2}{R_0}+\sum_{\{A,Z\}}N_{AZ}E_{AZ}, \tag{2}$$

where E_0^* is the total excitation energy, and $E_0^{\text{g.s.}}$ is ground-state energy of a nuclei having a mass and atomic number equal to that of the total system, A_0 and Z_0, respectively. The first term on the right-hand side stands for the Coulomb energy of a homogeneous charge Z_0e occupying the volume of the system of radius R_0, and N_{AZ} indicates the number of fragments of mass number A and atomic number Z in the partition of the system.

In the equation above, E_{AZ} is the kinetic plus internal energy for each of these fragments. It is related to the temperature by assuming all fragments are at a common temperature as follows:

$$E_{AZ}=\frac{3}{2}T+E_{AZ}^*(T)+E_{AZ}^C-B_{AZ}, \tag{3}$$

where the internal excitation energy of the fragments, $E_{AZ}^*(T)$, may be approximated by an extension of the semiempirical mass formula to finite temperatures [9], and the extra Coulomb energy of the fragment in the fragmentation volume, E_{AZ}^C, may be calculated within the Wigner-Seitz approximation. B_{AZ} stands for the ground-state binding energy for the fragment. Equations (2) and (3) result from an average of the microcanonical expression for energy conservation over the phase space corresponding to the specific decay partition.

By applying the energy conservation relationship in Eqs. (2) and (3), one obtains a temperature T that describes the internal excitation and translational energies of fragments within a given partition. Even though the overall system is assumed to be in equilibrium at a fixed excitation energy E_0^*, different decay partitions have different Coulomb, binding, and translational energies, and, consequently, different excitation energies of the emitted fragments. Consistency with Eqs. (2) and (3) therefore requires that the temperature T of the fragments varies from one decay partition to another, reflecting the differences between the Coulomb, binding and translational energies of the various partitions.

Labeling the partition $\{N_{AZ}\}$ with the index f, the statistical weight associated with the partition,

$$W_f=\exp\left[\sum_{\{A,Z\}}N_{AZ}S_{AZ}(T)\right], \tag{4}$$

may be found by expressing the entropy of the fragments, S_{AZ}, using approximations derived from the liquid drop model at finite temperature [9]. Consequently the physical observables can be expressed by a weighted average over decay partitions as

$$\langle O_{AZ}\rangle=\frac{\sum_f W_f O_{AZ}}{\sum_f W_f}, \tag{5}$$

where O_{AZ} can be any interesting observables such as the yield of a fragment or the temperature. (In the present work, the summation included 10^8 partitions.)

This allows one to predict the various results from the SMM that are addressed in Sec. III with regard to the temperature variations. Because the SMM approach invokes a temperature to sample the microcanonical phase space, we denote the predicted observables as *approximately* microcanonical. Despite this caveat, we note that this procedure can, in principal, give accurate microcanonical predictions for experimental observables provided the thermal expressions for the free energies are accurate descriptions of the integration over the microcanonical phase space.

Before passing on to the various results of our investigation, it is important to clarify that we do not invoke the grand canonical approximations to the SMM approach introduced in Ref. [17] to allow Monte Carlo event simulations [18,19]. Instead, we have adhered closely to original SMM approach outlined in Ref. [9], with the exception that all calculations in this paper were performed at a constant freezeout density equal to one-third that of the saturation density of nuclear matter.

III. PRIMARY TEMPERATURES

The SMM procedure expressed in Eqs. (2)–(5) leads to a distribution of the temperatures of the fragmenting system for a given excitation energy in the same sense that the temperature of the daughter nucleus in compound nuclear decay theory varies as a function of the Coulomb barrier and separation energy of each decay channel. The points in Fig. 1 denote the temperature distributions for the fragmentation of an excited ^{112}Sn nucleus at three different excitation energies obtained with the SMM. These distributions are well fitted by Gaussian functions, shown by the curves in the figure, with variances σ_T^2 that are fairly independent of the energy, $\sigma_T \approx 0.4$ MeV, in the range 3 MeV$\leqslant E_0^*/A \leqslant$10 MeV. At each excitation energy, we average over all of the partitions and define this average value as the ''approximate microcanonical'' temperature T_{MIC}.

Since each of the isotopes employed in the thermometer has a specific mass, charge, and binding energy, the applica-

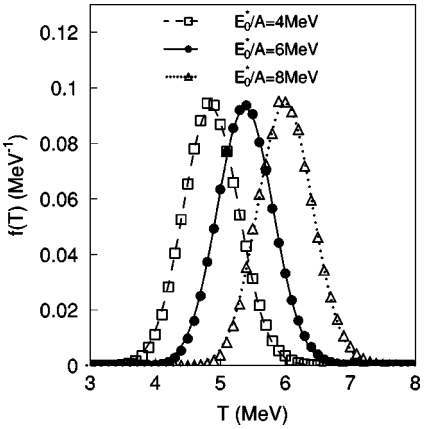

FIG. 1. The points denote distributions of temperatures calculated with the SMM approach for the decay of a ^{112}Sn nucleus at three different excitation energies. The lines denote Gaussian fits to the calculated distributions.

tion of conservation laws sets a constraint on the values available to the remainder of the system. Because of this finite-size effect, the temperature distribution obtained when a specific isotope is present is slightly different from the one obtained when all partitions are considered. In particular, a small difference ($\leqslant$0.1 MeV) is observed between the average temperatures for the various isotopes; this is illustrated in Fig. 2 for carbon isotopes from the fragmentation of a ^{112}Sn nucleus at $E_0^*/A=6$ MeV. Even though the average temperatures are different reflecting the different binding energies of the three isotopes, all these distributions are Gaussians with nearly the same variances. We can extract another temperature T_{IMF} by averaging over partitions which contain an intermediate mass fragment (IMF) with $3\leqslant Z\leqslant 10$. It's interesting to note that T_{MIC} can exceed T_{IMF} at low energies by as much as 0.2 MeV, in part because it takes more energy to emit an IMF than to emit an equivalent mass in the form of α particles, leaving less energy for thermal excitation.

The basic idea contained in Eq. (1) was derived under the

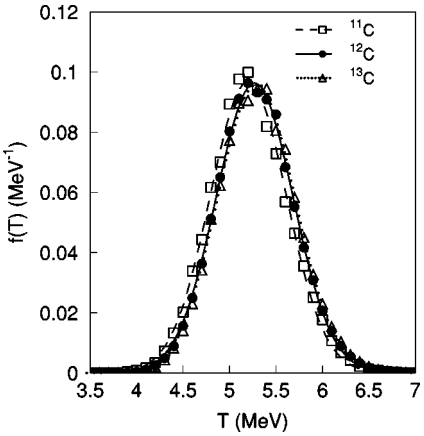

FIG. 2. The points denote temperature distributions calculated with the SMM approach for the different isotopes considered in the carbon thermometer for an excitation energy of $E_0^*/A=6$ MeV. The lines denote Gaussian fits to the calculated distributions.

assumption that the primary yields are well represented by the grand canonical approximation at a single breakup temperature; the double ratio was invoked to cancel out the contribution to the yields coming from the neutron and proton chemical potentials. In the SMM, however, the temperature varies from partition to partition and the chemical potentials, which appear within the grand canonical formalism as Lagrange multipliers that conserve charge and mass, are not explicitly invoked. Thus, we can not presume the validity of the Albergo's formula [Eq. (1)] in the SMM, and must test its validity instead.

We begin with a test of the validity of Eq. (1) when one employs the primary yields. For a given decay partition $\{N_{AZ}\}$, we take into account the internal free energy $F_{AZ}^{\rm int}(T)$, which is parametrized as

$$F_{AZ}^{\rm int}=-B(A,Z)+F_{AZ}^*(T)+F_{AZ}^C, \tag{6}$$

$$F_{AZ}^*(T)=F_{AZ}^{B*}(T)+F_{AZ}^{S*}(T)-T\ln(g_{AZ}^{\rm g.s.}), \tag{7}$$

where $g_{AZ}^{\rm g.s.}$ is the ground-state spin degeneracy, and F_{AZ}^{B*}, F_{AZ}^{S*}, and F_{AZ}^C correspond to the excitation energy-dependent bulk, surface, and Coulomb contributions to the internal free energy [20] after the binding energy part has been removed. The reader is referred to Ref. [9] for explicit expressions for the terms entering in the equation above. Then the primary yield for the ground state can be related to the total yield by

$$N_{AZ}^{\rm g.s.}=N_{AZ}\cdot g_{AZ}^{\rm g.s.}\exp[F_{AZ}^*(T)/T] \tag{8}$$

for this partition. Following the procedure described in Sec. II, we will use this expression and Eq. (5) to obtain the average ground-state yield distribution $\langle N_{AZ}^{\rm g.s.}\rangle$. This, in turn, can be used in Eq. (1) to extract isotopic temperatures as follows:

$$\frac{\langle N_{A1,Z1}^{\rm g.s.}\rangle/\langle N_{A1+1,Z1}^{\rm g.s.}\rangle}{\langle N_{A2,Z2}^{\rm g.s.}\rangle/\langle N_{A2+1,Z2}^{\rm g.s.}\rangle}=C\exp\left(\frac{\Delta B}{T_{iso}^{smm}}\right). \tag{9}$$

In previous SMM calculations, experimental binding energies and spin degeneracy factors $g_{AZ}^{\rm g.s.}$ were used for light nuclei with $A<5$. Liquid drop binding energies and spin degeneracy factors of unity were used for $A\geqslant 5$. In this work, we will retain these conventions on spin degeneracy factors so as to be consistent with prior calculations, but we will use empirical binding energies for all nuclei.

In Fig. 3, the isotopic temperatures T_{iso}^{smm} for the carbon thermometer ($Z_1=Z_2=6$, $A_1=11$, and $A_2=12$) are plotted as the stars for the multifragmentation of a ^{112}Sn source at excitation energies $E_0^*/A=3$–10 MeV. For comparisons, the corresponding T_{MIC} and T_{IMF} for the same system are also shown in Fig. 3 as dashed and solid lines, respectively. While supporting the concept of isotopic thermometry, the good agreement between T_{IMF} and T_{iso}^{smm} is somewhat surprising, given the strong dependence of the Boltzmann factor on temperature for large ΔB and the width of the temperature distribution shown in Fig. 1. As shown in Sec. IV, this occurs in part due to a large cancellation involving the Boltzmann factor and the temperature dependencies of the effec-

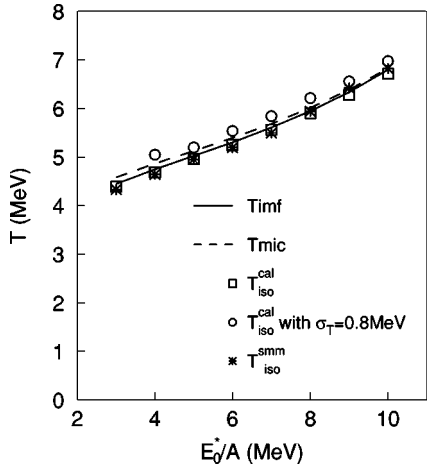

FIG. 3. Comparisons of various primary temperatures T_{MIC}, T_{IMF}, and T_{iso}^{smm} from the SMM calculation, and T_{iso}^{cal} from the analytical calculation in the grand canonical limit. For details, see the text. One point is missing for T_{iso}^{cal} with $\sigma_T=0.8$ MeV, because the calculated value for p for the correction term in Eq. (12) becomes negative at $E_0^*/A=3$ MeV, i.e., the expansion breaks down in this case.

tive chemical potentials. Figure 3 also reveals that fairly precise information about T_{IMF} and somewhat less precise information about T_{MIC} are provided by the primary yields. This suggests that given a precise relationship between primary to final yields, it would be possible to determine the breakup temperature from the measured yields.

IV. EFFECTS OF TEMPERATURE VARIATIONS

The surprising consistency between T_{IMF} and T_{iso}^{smm} in Fig. 3 suggests that the corrections to the grand canonical prediction for the isotope temperatures are small, and one may utilize this approach to understand why the temperature variations have so little influence on the results. Taking this tack, we assume that the isotopic distributions are well approximated for each partition by the grand canonical limit, use this limit to gain insight into the finite size effects, and at the same time investigate the accuracy of this approximation. We take this approach to consider, first, the influence of the temperature variations and later the consequences of the finite size on the effective chemical potentials.

Considering the influence of the temperature variations in this approximation, we average the grand canonical approximation over the temperature distribution in Fig. 1. If the approximation works, the expressions that result from this average should be appropriate for the consideration of the effects of temperature distributions arising from other effects, and within other equilibrium models of multifragmentation as well. Taking this approach, the yield of a particular isotope i in the framework of Albergo's method [15], when averaged over all possible partitions, becomes

$$\langle Y_i\rangle = V\int_0^\infty dT\, f(T)\frac{A_i^{3/2}\zeta_i(T)}{\lambda_T^3} \times \exp[(Z_i\,\mu_{PF}(T)+N_i\,\mu_{NF}(T)+B_i)/T], \quad (10)$$

where $f(T)$ is the temperature distribution, V represents the free volume of the system, $\lambda_T=\sqrt{2\pi\hbar^2/mT}$, m is the nucleon mass, and μ_{PF} (μ_{NF}) stands for the chemical potential associated with free protons (neutrons) at temperature T. The internal partition function of the fragment i is given by

$$\zeta_i(T)=\sum_j g_i^j \exp\left[-\frac{\Delta E_j}{T}\right], \quad (11)$$

where ΔE_j is the excitation energy of the state j with respect to the ground state, and g_i^j stands for the spin degeneracy factor of this excited state.

Assuming that $f(T)$ is a Gaussian centered at $\langle T\rangle$ and with width $\sigma_T \ll \langle T\rangle$ (see Fig. 1), one may expand $1/T$, and $T^{3/2}$ and the chemical potentials. By considering only fragments observed in the ground state, i.e., $\zeta_i(T)=g_i^0$, we obtain that

$$\langle Y_i^{\text{g.s.}}\rangle = \frac{g_i^0 V A_i^{3/2}\langle T\rangle^{3/2}}{\lambda_*^3} \times\exp\left[\frac{B_i}{\langle T\rangle}+\frac{\mu_{PF}(\langle T\rangle)Z_i+\mu_{NF}(\langle T\rangle)N_i}{\langle T\rangle}\right] \times\frac{1}{\sqrt{2p}}\cdot\exp\left[\frac{q^2}{4p}\right], \quad (12)$$

where $\lambda_*\equiv\sqrt{2\pi\hbar^2/m}$. In the above expression, the corrections to the grand canonical relationship are provided by the correction factor $1/\sqrt{2p}\,\exp[q^2/4p]$ which depends on the assumed width of the temperature distribution and the binding energy of the ith fragment, as well as the neutron and proton chemical potentials and their derivatives through the parameters p and q. These two parameters are defined by

$$p=\frac{1}{2}+\left[\frac{\sigma_T}{\langle T\rangle}\right]^2\left[Z_i\alpha_{PF}+N_i\alpha_{NF}+\frac{3}{4}-\frac{B_i}{\langle T\rangle}\right], \quad (13)$$

$$q=\frac{\sigma_T}{\langle T\rangle}\left(Z_i\beta_{PF}+N_i\beta_{NF}+\frac{3}{2}-\frac{B_i}{\langle T\rangle}\right),$$

where

$$\alpha_{PF}=\mu'_{PF}(\langle T\rangle)-\frac{\mu_{PF}(\langle T\rangle)}{\langle Tt\rangle}-\frac{1}{2}\mu''_{PF}(\langle T\rangle)\langle T\rangle, \quad (14)$$

$$\beta_{PF}=\mu'_{PF}(\langle T\rangle)-\frac{\mu_{PF}(\langle T\rangle)}{\langle T\rangle},$$

$$\alpha_{NF}=\mu'_{NF}(\langle T\rangle)-\frac{\mu_{NF}(\langle T\rangle)}{\langle T\rangle}-\frac{1}{2}\mu''_{NF}(\langle T\rangle)\langle T\rangle,$$

$$\beta_{NF}=\mu'_{NF}(\langle T\rangle)-\frac{\mu_{NF}(\langle T\rangle)}{\langle T\rangle}.$$

The isotopic temperature can be extracted from the above corrected yields. Replacing $Y(A,Z)$ in Eq. (1) by the right-

hand side of Eq. (12), one cancels out the spin- and mass-dependent term C, and then obtains

$$\exp[\Delta B/T_{iso}^{cal}]=\frac{G(A_1,Z_1)/G(A_1+1,Z_1)}{G(A_2,Z_2)/G(A_2+1,Z_2)}, \tag{15}$$

where

$$G(A,Z)=\exp\left[\frac{B_i}{\langle T\rangle}+\frac{\mu_{PF}(\langle T\rangle)Z+\mu_{NF}(\langle T\rangle)N}{\langle T\rangle}\right]$$

$$\times\frac{1}{\sqrt{2p}}\exp\left[\frac{q^2}{4p}\right]. \tag{16}$$

In the above double ratio the terms involving the chemical potentials evaluated at the average temperature cancel; however, terms in the correction factor involving the derivatives of the chemical potentials remain.

Quantitative estimates of the correction factor require one to obtain estimates for the effective chemical potentials and their derivatives with respect to temperature. The proton and neutron chemical potentials at temperature T may be calculated from the free proton and neutron multiplicities via the expressions

$$\mu_{PF}(T)=T\ln\left[\frac{\lambda_T^3 Y_{PF}(T)}{g_{PF}V}\right], \tag{17}$$

$$\mu_{NF}(T)=T\ln\left[\frac{\lambda_T^3 Y_{NF}(T)}{g_{NF}V}\right],$$

where g_{PF} (g_{NF}) represents the spin degeneracy factor of the proton (neutron). For the calculations presented in this work, it has proven advantageous and reasonably accurate to approximate the yields $Y_{PF}(T)$ and $Y_{NF}(T)$ over a modest range in temperature by power-law expressions in the temperature. In this approximation,

$$Y_{PF}(T)=c_{PF}T^{\gamma_{PF}}, \tag{18}$$

$$Y_{NF}(T)=c_{NF}T^{\gamma_{NF}}.$$

For the decay of ^{112}Sn nuclei at temperatures ranging over $4\leqslant T\leqslant 7$ MeV, Y_{PF} and Y_{NF} are well described by $\gamma_{PF}=4.5$ and $\gamma_{NF}=1.0$ ($c_{PF}=1.33\times10^{-4}$ and $c_{NF}=0.267$) according to the SMM; comparisons of this parametrization to yields calculated with the SMM model are shown in Fig. 4. These values depend on the density, which has been chosen to be one-third that of the saturation density of nuclear matter. Larger values of the free nucleon yields are obtained at lower density.

Using this approximation, the explicit forms of the correction factors in Eqs. (12)–(14) become $2\alpha_{PF}=\beta_{PF}=(\gamma_{PF}-\frac{3}{2})=3$ and $2\alpha_{NF}=\beta_{NF}=(\gamma_{NF}-\frac{3}{2})=-\frac{1}{2}$. We note that the correction factor to the temperature T_{iso}^{cal} in Eq. (15) depends on the power-law exponents γ_{PF} (γ_{NF}), and not on the absolute values of the proton (neutron) yields.

Even though Eq. (10) has an exponent that appears to be strongly temperature dependent, there is a strong cancellation between the contributions from the chemical potentials and binding-energy factors in the expressions for p and q. As a result, the correction factor is of order unity. Values in the range of $1/\sqrt{2p}\exp[q^2/4p]\approx 1-2$ are obtained, for example, in the decay of ^{112}Sn nuclei at temperatures in the range of $4\leqslant T\leqslant 7$ MeV.

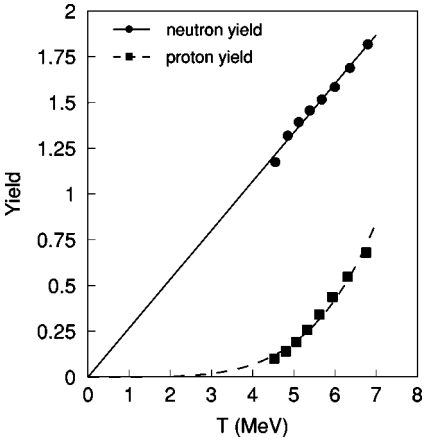

FIG. 4. The solid squares and circles denote the free proton and neutron yields, respectively, calculated via the SMM approach. The solid and dashed lines denote fits to the calculated yields following Eq. (18).

The isotopic temperatures T_{iso}^{cal} calculated from Eq. (15) for carbon thermometer are shown in Fig. 3 in comparisons with temperatures T_{MIC}, T_{IMF}, and T_{iso}^{smm} derived from the SMM in the previous session. The very good agreement between T_{iso}^{cal}, T_{iso}^{smm}, and T_{IMF} indicates that the corrections to the isotopic temperatures associated with these temperature variations are small, although the yields can change by as much as a factor of 2. This comparative insensitivity arises because the isotopic thermometers depend logarithmically on the yields.

This insensitivity depends on the nature and magnitude of the temperature variation. The corrections to the isotopic temperatures will be somewhat larger in other contexts or other models where the temperature variations are larger. The limited precision with which systems may be selected experimentally may also have a similar influence, because the excitation energy and temperature varies experimentally from collision to collision due to variations in the impact parameter or in the energy removed by preequilibrium particle emission. The influence of this temperature variation, which may exceed the variation in temperature caused by the averaging over decay partitions, can also be estimated via techniques outlined in the present section. To illustrate how one can estimate the possible corrections due to an imprecision in the excitation energy definition, the circles in Fig. 3 show calculations using Eq. (15) for the carbon thermometer, assuming a width of $\sigma_T\approx 0.8$ MeV for the temperature distribution, which is twice as large as that predicted in Figs. 1 and 2. This width is not based upon a dynamical calculation; it is only to illustrate that larger isotopic temperatures can result if the excitation energy is poorly defined.

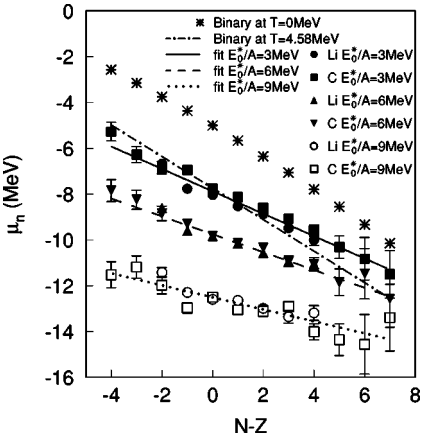

FIG. 5. The squares, circles, and triangles denote neutron chemical potentials derived from Eq. (19) using SMM predictions for carbon and lithium isotopic yields at various initial excitation energies for the decay of the nucleus ^{112}Sn. The stars and the dot-dashed line denote approximate values calculated from Eq. (23) for $T=0$ and 4.58 MeV, respectively. The error bars denote the statistical errors in the calculation, which in many cases are too small to be observed in the figure.

V. CHEMICAL POTENTIALS

The grand canonical limit has a great advantage of providing a simple analytical expression for the isotopic yields from which other useful expressions can be derived. However, the concept of uniform chemical potentials is not a prediction of microcanonical or canonical models, and must be investigated to determine its applicability to finite systems. We do this by trying to compare the grand canonical expression for the isotopic yields to the predictions of approximately microcanonical SMM calculations. We start by assuming that these isotopic distributions can be calculated within the grand canonical approximation, and then test this assumption as follows. Using a pair of adjacent isotopes, we invert the grand canonical expression for the isotopic yields of two adjacent isotopes, to obtain an equation for the *effective* neutron chemical potential,

$$\mu_n^{eff}(A,Z)=T\ln\left[\frac{g_{AZ}^{\text{g.s.}}}{g_{A+1Z}^{\text{g.s.}}}\left(\frac{A}{A+1}\right)^{3/2}\times\exp[(B_{AZ}-B_{A+1Z})/T]\frac{Y_{A+1Z}^{\text{g.s.}}}{Y_{AZ}^{\text{g.s.}}}\right], \quad (19)$$

where $g_{AZ}^{\text{g.s.}}$, B_{AZ}, and $Y_{AZ}^{\text{g.s.}}$ are the ground-state spin degeneracy, the binding energy, and the ground-state primary yield for a fragment with (A,Z), respectively. If the $Y_{AZ}^{\text{g.s.}}$ taken to be the ground state yields predicted by the SMM, $\mu_n^{eff}(A,Z)$ becomes an effective ''SMM'' chemical potential. By performing SMM calculations, we find the temperature and isotopic dependencies of the effective neutron chemical potentials given in Fig. 5 for carbon and lithium isotopes from the decay of a ^{112}Sn nucleus at excitation energies of $E_0^*/A=3$, 6, and 9 MeV.

These effective chemical potentials are essentially the same for the carbon and lithium isotope chains. This insensitivity to element number is consistent with the concept of a chemical potential, and offers support for the use of the grand canonical expression to describe isotopic distributions. There is a dependence on the neutron number of the isotope, however, that lies outside of the grand canonical approximation. This variation in the neutron chemical potential basically comes as a result of mass, charge, and energy conservation for a finite-size system. We can understand the influence of these conservation laws most easily at low excitation energies, where the two largest fragments in the final state are the IMF (carbon or lithium in this case) and a heavy residue which contains most of the remaining charge and mass. We estimate the influence of conservation laws at low excitation energy qualitatively by considering binary decay configurations. Assuming that a parent nucleus (A_0,Z_0) decays into a light fragment (A,Z) and a heavy residue (A_0-A,Z_0-Z), we can approximate the yield of fragment (A,Z) in its ground state by

$$\begin{aligned}Y_{AZ}^{\text{g.s.}}&\propto\rho^{\text{g.s.}}(A,Z)\rho^*(A_0-A,Z_0-Z)\overline{\rho}_{REL}\\&\approx g_{AZ}^{\text{g.s.}}\exp[S^*(A_0-A,Z_0-Z)]\\&\quad\times\left[\frac{A\cdot(A_0-A)}{A_0}\right]^{3/2}\frac{1}{\lambda_T^3},\end{aligned} \quad (20)$$

where $\rho^{\text{g.s.}}=g_{AZ}^{\text{g.s.}}$, ρ^*, and S^* are the density of states for the light nucleus in its ground-state level, and the density of states and entropy of the heavy residue in its excited state, respectively. The other factor, $\overline{\rho}_{REL}\approx[A(A_0-A)/A_0]^{3/2}\lambda_T^{-3}$, is the thermal average of the state density of relative motion.

Replacing the yields in Eq. (19) with Eq. (20), and assuming $A\ll A_0$, one finds that the effective chemical potential depends on the difference in residue entropies, $S^*(A_0-A-1,\overline{Z})-S^*(A_0-A,Z_0-Z)$. Using an expansion for small changes in the nuclear entropy from Ref. [16], this difference can be expressed in terms of the difference of binding energies,

$$\begin{aligned}&S^*(A_0-A-1,\overline{Z})-S^*(A_0-A,Z_0-Z)\\&\quad=-(B_{A_0-A,Z_0-Z}-B_{A_0-A-1,Z_0-Z})/T\\&\quad\quad-(B_{AZ}-B_{A+1Z})/T+f^*/T,\end{aligned} \quad (21)$$

plus a term depending on the free excitation energy per nucleon: $f^*=E^*/A_0-TS/A_0$. This difference in binding energies is further related to the neutron separation energy $s_n(A_0-A,Z_0-Z)$:

$$s_n(A_0-A,Z_0-Z)=B_{A_0-A,Z_0-Z}-B_{A_0-A-1,Z_0-Z}. \quad (22)$$

One consequently obtains the following expression for the effective chemical potential,

$$\mu_n=-s_n(A_0-A,Z_0-Z)+f^*, \quad (23)$$

where the reduced free excitation energy has been approximated by its low-energy limit

$$f^* = -\frac{T^2}{\varepsilon_0}, \quad \varepsilon_0 = 8 \text{ MeV}. \tag{24}$$

For the decay $^{112}\text{Sn} \rightarrow ^{12}\text{C} + X$, the chemical potential at $T = 0$, i.e., $-s_n(A_0 - A, Z_0 - Z)$, is plotted as the stars in Fig. 5; the binding energies for these calculations were calculated using the liquid-drop parametrization in Ref. [21]. The reduced free energy f^* gives a reasonable estimate for the trend with excitation energy. The dot-dashed line in Fig. 5 gives the chemical potential predicted from Eq. (23) for $E_0^*/A = 3$ MeV ($T = 4.58$ MeV). The predicted trend is close to that predicted by the SMM model (solid circles and squares), but has a somewhat stronger dependence on $N - Z$.

In general, the slope of the effective neutron chemical potential becomes slightly flatter as the excitation energy or temperature increases. If we consider that the system undergoes a multiple fragment decay at higher temperatures, it is clear that approximating the entropy of the remaining system by that of a residue of comparable mass becomes rather inaccurate. The constraints imposed on the total system by the isospin asymmetry of one observed fragment should, in that case, be less significant. While there is a mass dependence to the effective chemical potential that is inconsistent with the grand canonical approach, it is useful to note that the mass dependence of the chemical potential (for these systems of more than 100 nucleons) is small if one is mainly concerned with nuclei near the valley of stability. If one cancels the chemical potential effects by constructing double ratios like that of the Algergo formula, the consequence of such finite-size effects becomes negligible indeed.

VI. INFLUENCE OF SECONDARY DECAY

As discussed in Sec. II, fragments are formed in excited states as well as in their ground states, corresponding to the breakup temperature. Fragments in short-lived excited states decay before they are detected and, therefore, the observed yields differ from that of the primary fragments. The effects of secondary decay on the isotopic yields and isotopic temperatures have already been reported by some authors (see, for example, Refs. [22–24]). Although the approaches employed in the description of the decay of hot primary fragments are different, all those works qualitatively agree on the point that the isotopic temperature is lower than the thermodynamical one.

At the quantitative level, details of the population and decay of the excited fragments are important. One issue concerns the importance of utilizing empirical binding energies, energy levels, and decay branching ratios for the excited fragments. Figure 6 shows the primary and secondary carbon isotopic distributions for the decay of a ^{112}Sn nucleus at initial excitation energies of $E_0^*/A = 4$ and 6 MeV. The primary distribution (solid line) is calculated by considering empirical binding energies within the SMM for hot fragments. The simplified Weisskopf evaporative decay procedure of Ref. [17] is used for one final distribution (dotted line). The other final distribution (dashed line) is obtained by calculating the secondary decay for $Z \leqslant 10$ hot fragments, as in Refs. [24,25], according to empirical nuclear structure information regarding the excitation energies, spins, isospins, and decay branching ratios where available. For hot fragments with $Z \leqslant 10$, where such information is not available, the decay is calculated according to the Hauser-Feshbach formalism [26]. The contributions to this latter calculation, from the secondary decay of hot fragments with $Z > 10$, are calculated, for simplicity, via the secondary evaporative decay procedure of Ref. [17]. Decays of fragments with $Z > 10$ make a 15% contribution to the yields of ^{12}C isotopes that may be altered when the decay of hot fragments with $Z > 10$ is calculated more accurately.

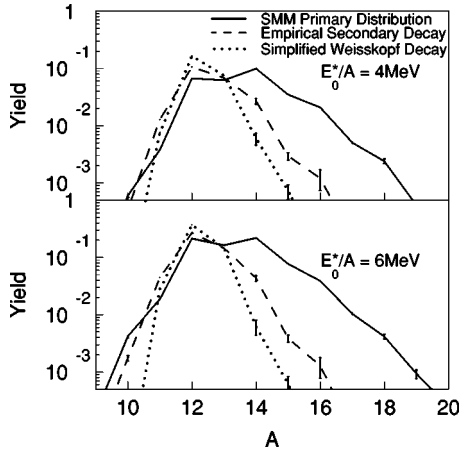

FIG. 6. Primary (solid line) and final carbon isotopic distributions calculated for the decay of the nucleus ^{112}Sn using (dashed line) and neglecting (dotted line) the empirical nuclear structure information in the secondary decay process. The error bars denote the statistical errors in the calculation, which in many cases are too small to be observed in the figure.

Obviously, in Fig. 6, the final distribution after the empirical secondary decay is much wider than the final distribution obtained via the evaporative decay approach of Ref. [17]. This points out the importance of using the empirical information in such calculations. This also leads to the extraction of larger isotopic temperatures via Eq. (1) for the empirical approach. Temperatures for the carbon isotope thermometer and He-Li thermometer calculated for the two secondary decay approaches are shown, for example, in Fig. 7 for the multifragmentation of a ^{112}Sn nucleus at $E_0^*/A = 4$–10 MeV. For reference, the curves T_{MIC} and T_{IMF} from Fig. 3 are also shown as the dashed and solid lines in the figure. Clearly, incorporating empirical information in the decay makes a significant difference. Both calculations provide lower isotopic temperatures than have been obtained in recent experiments [7,8,13,14].

It should be noted, however, that the simplified Weisskopf evaporative decay, shown in Figs. 6 and 7, is only used in the SMM code of Ref. [17] to calculate the decay of fragments with $A > 16$. The decay of lighter fragments is calculated via a ''Fermi breakup'' multiparticle decay formalism. This latter decay mechanism makes the dominant contribution to the

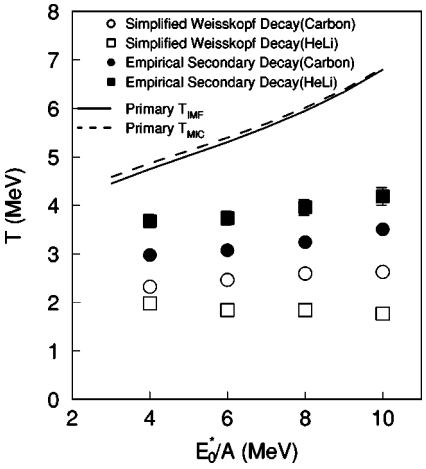

FIG. 7. Isotopic temperatures for carbon and He-Li thermometers calculated with the SMM model for the decay of the nucleus ^{112}Sn using (solid symbols) and neglecting (open symbols) the empirical nuclear structure information in the secondary decay process. The lines are the same as those shown in Fig. 3. The error bars denote the statistical errors in the calculation, which in many cases are too small to be observed in the figure.

isotope temperatures calculated via the latter SMM code in Ref. [27]. Investigations of the experimental and theoretical basis for the Fermi breakup approach are needed, but are out of the scope of the present work.

Regardless of the decay formalism, memory of the breakup stage is lost via the secondary decay mechanism. The degree of memory loss depends on the details of the secondary decay correction and on the role of short-lived higher-lying particle unbound states. A smaller degree of memory loss ensues in models such as those of Refs. [10,28,29], where few, if any, particle unbound states are considered. The approach of Ref. [17] represents the other extreme, wherein all states are considered regardless of lifetime. This issue clearly needs further study to see whether the role of particle unstable nuclei can be constrained, for example, by direct measurements using techniques discussed in Refs. [25,30] or by other experimental observables.

VII. CONCLUDING REMARKS

We discussed some of main aspects that could cause microcanonical predictions for isotopic distributions and isotopic temperatures to differ from grand canonical calculations, and influence the determination of the breakup temperature and other experimental observables. We investigate this problem by checking the consistency of the grand canonical expression for the isotopic yields against the approximately microcanonical SMM predictions, and explore the potential role which may be played by variations in the temperature and in the effective chemical potentials. These variations occur as a consequence of the finite size of the disintegrating system, and are therefore present in all microcanonical calculations.

Concerning the temperature variation, we find that this causes the isotopic yields obtained with the approximately microcanonical SMM simulations for the primary distribution to differ from those of the grand canonical ensemble by factors of order unity. One difference stems from the averaging over the temperatures corresponding to the different breakup partitions. These vary because the total binding, Coulomb, and translational kinetic energies vary from partition to partition, and, by subtraction, the thermal energy must vary as well. A simple and relatively accurate prescription that accounts for these temperature variations was given that may also prove useful for estimating the influence of thermal averaging over the variations in the actual excitation energy deposition within a data set that is constrained by an experimental cut on the estimated energy deposition.

We also extract effective chemical potentials by comparing approximate microcanonical and grand canonical expressions for the isotopic yields. These effective chemical potentials are approximately the same for isotopes of different elements that lie along the valley of β stability, but vary as a function of $(N\text{-}Z)$. For example, for the neutron chemical potential we observe a dependence upon $(N\text{-}Z)$ that can be understood at low excitation energies to arise from the dependence of the neutron separation energy on the location of the accompanying residue relative to the line of β stability.

Typically, these variations in temperature and effective chemical potential cause variations in the isotopic yields of order unity. The logarithmic relation between the isotopic temperature and the yields means that the latter may be wrongly predicted by a factor of 2, and one may still find a reasonable agreement between the approximate microcanonical and the isotopic temperatures provided the binding-energy difference ΔB is significantly larger than the temperature. When the effects of secondary decay is taken into account, however, the yields can change by more than an order of magnitude, and the temperature values can decrease appreciably. While the magnitude of this change is not yet unambiguously established, it was shown that the incorporation of empirical information about the decay is essential for quantitative comparisons to experimental data. Measurements that quantify the role of higher-lying particle unstable states are essential for determining the magnitude of these secondary decay corrections.

ACKNOWLEDGMENTS

We would like to acknowledge important discussions with Alexander Botvina and HongFei Xi during the early stages of this work. R.D. and S.R.S. thank the NSCL at MSU for support during visits on which part of this work was performed, and also the MCT/FINEP/CNPq (PRONEX) program, under Contract No. 41.96.0886.00, CNPq, FAPERJ, and FUJB for partial financial support. This work was supported in part by the National Science Foundation under Grant No. PHY-95-28844.

[1] G. Baym and Ch. Pethick, *Landau-Fermi Liquid Theory* (Wiley, New York, 1991).

[2] H. Jaqaman, A. Z. Mekjian, and L. Zamick, Phys. Rev. C **27**, 2782 (1983).

[3] Horst Müller and Brian D. Serot, Phys. Rev. C **52**, 2072 (1995).

[4] C. Williams, W. G. Lynch, C. Schwarz, M. B. Tsang, W. C. Hsi, M. J. Huang, D. R. Bowman, J. Dinius, C. K. Gelbke, D. O. Handzy, G. J. Kunde, M. A. Lisa, C. F. Peaslee, L. Phair, A. Botvina, M-C. Lemaire, S. R. Souza, C. Van Buren, R. J. Charity, L. G. Sobotka, U. Lynen, I. Pochodzalla, H. Sann, W. Trautmann, D. Fox, R. T. de Souza, and N. Carlin, Phys. Rev. C **55**, R2132 (1997).

[5] A. Schuttauf, W. D. Kunze, A. Worner, M. Begemann-Blaich, Th. Blaich, D. R. Bowman, R. J. Charity, A. Cosmo, A. Ferrero, C. K. Gelbke, C. Gross, W. C. Hsi, J. Hubele, G. Imme, I. Iori, J. Kempter, P. Kreutz, G. J. Kunde, V. Lindenstruth, M. A. Lisa, W. G. Lynch, U. Lynen, M. Mang, T. Mohlenkamp, A. Moroni, W. F. J. Muller, M. Neumann, B. Ocker, C. A. Ogilvie, G. F. Peaslee, J. Pochodzalla, G. Raciti, F. Rosenberger, Th. Rubehn, H. Sann, C. Schwarz, W. Seidel, V. Serfling, L. G. Sobotka, J. Stroth, L. Stuttge, S. Tomasevic, W. Trautmann, A. Trzcinski, M. B. Tsang, A. Tucholski, G. Verde, C. W. Williams, E. Zude, and B. Zwieglinski, Nucl. Phys. **A607**, 457 (1996).

[6] Walter Benenson, David J. Morrissey, and William A. Friedman, Annu. Rev. Nucl. Part. Sci. **44**, 27 (1994), and references therein.

[7] J. Pochodzalla, T. Mohlenkamp, T. Rubehn, A. Schuttauf, A. Worner, E. Zude, M. Begemann-Blaich, Th. Blaich, H. Emling, A. Ferrero, C. Gross, G. Imme, I. Iori, G. J. Kunde, W. D. Kunze, V. Lindenstruth, U. Lynen, A. Moroni, W. F. J. Muller, B. Ocker, G. Raciti, H. Sann, C. Schwarz, W. Seidel, V. Serfling, J. Stroth, W. Trautmann, A. Trzcinski, A. Tucholski, G. Verde, and B. Zwieglinski, Phys. Rev. Lett. **75**, 1040 (1995).

[8] M. J. Huang, H. Xi, W. G. Lynch, M. B. Tsang, J. D. Dinius, S. J. Gaff, C. K. Gelbke, T. Glasmacher, G. J. Kunde, L. Martin, C. P. Montoya, E. Scannapieco, P. M. Milazzo, M. Azzano, G. V. Margagliotti, R. Rui, G. Vannini, N. Colonna, L. Celano, G. Tagliente, M. D'Agostino, M. Bruno, M. L. Fiandri, F. Gramegna, A. Ferrero, I. Iori, A. Moroni, F. Petruzzelli, and P. F. Mastinu, Phys. Rev. Lett. **78**, 1648 (1997).

[9] J. P. Bondorf, R. Donangelo, I. N. Mishustin, C. J. Pethick, H. Schulz, and K. Sneppen, Nucl. Phys. **A443**, 321 (1985); **A444**, 460 (1985); **A448**, 753 (1986).

[10] D. H. E. Gross, Phys. Rep. **279**, 119 (1997).

[11] Y.-G. Ma, A. Siwek, J. Peter, F. Gulminelli, R. Dayras, L. Nalpas, B. Tamain, E. Vient, G. Auger, Ch. O. Bacri, J. Benlliure, E. Bisquer, B. Borderie, R. Bougault, R. Brou, J.-L. Charvet, A. Chbihi, J. Colin, D. Cussol, E. De Filippo, A. Demeyer, D. Dore, D. Durand, P. Ecomard, P. Eudes, E. Gelic, D. Gourio, D. Guinet, R. Laforest, P. Lautesse, J. L. Laville, L. Lebreton, J. F. Lecolley, A. Le Fevre, T. Lefort, R. Legrain, O. Lopez, M. Louvel, J. Lukasik, N. Marie, V. Metivier, A. Ouatizerga, M. Parlog, E. Plagnol, A. Rahmani, T. Reposeur, M. F. Rivet, E. Rosato, F. Saint-Laurent, M. Squalli, J. C. Steckmeyer, M. Stern, L. Tassan-Got, C. Volant, and J. P. Wieleczko, Phys. Lett. B **390**, 41 (1997).

[12] J. A. Hauger, P. Warren, S. Albergo, F. Bieser, F. P. Brady, Z. Caccia, D. A. Cebra, A. D. Chacon, J. L. Chance, Y. Choi, S. Costa, J. B. Elliott, M. L. Gilkes, A. S. Hirsch, E. L. Hjort, A. Insolia, M. Justice, D. Keane, J. C. Kintner, V. Lindenstruth, M. A. Lisa, H. S. Matis, M. McMahan, C. McParland, W. F. J. Müller, D. L. Olson, M. D. Partlan, N. T. Porile, R. Potenza, G. Rai, J. Rasmussen, H. G. Ritter, J. Romanski, J. L. Romero, G. V. Russo, H. Sann, R. P. Scharenberg, A. Scott, Y. Shao, B. K. Srivastava, T. J. M. Symons, M. Tincknell, C. Tuvé, S. Wang, H. H. Wieman, T. Wienold, and K. Wolf, Phys. Rev. C **57**, 764 (1998).

[13] V. Serfling, C. Schwarz, R. Bassini, M. Begemann-Blaich, S. Fritz, S. J. Gaff, C. Groß , G. Immé, I. Iori, U. Kleinevoß , G. J. Kunde, W. D. Kunze, U. Lynen, V. Maddalena, M. Mahi, T. Möhlenkamp, A. Moroni, W. F. J. Müller, C. Nociforo, B. Ocker, T. Odeh, F. Petruzzelli, J. Pochodzalla, G. Raciti, G. Riccobene, F. P. Romano, A. Saija, M. Schnittker, A. Schüttauf, W. Seidel, C. Sfienti, W. Trautmann, A. Trzcinski, G. Verde, A. Wörner, Hongfei Xi, and B. Zwieglinski, Phys. Rev. Lett. **80**, 3928 (1998).

[14] H. F. Xi, G. J. Kunde, O. Bjarki, C. K. Gelbke, R. C. Lemmon, W. G. Lynch, D. Magestro, R. Popescu, R. Shomin, M. B. Tsang, A. M. Vandermolen, G. D. Westfall, G. Imme, V. Maddalena, C. Nociforo, G. Raciti, G. Riccobene, F. P. Romano, A. Saija, C. Sfienti, S. Fritz, C. Groß, T. Odeh, C. Schwarz, A. Nadasen, D. Sisan, and K. A. G. Rao, Phys. Rev. C **58**, 2636 (1998).

[15] S. Albergo, S. Costa, E. Costanzo, and A. Rubbino, Nuovo Cimento **89**, 1 (1985).

[16] W. A. Friedman and W. G. Lynch, Phys. Rev. C **28**, 950 (1983).

[17] A. S. Botvina, A. S. Iljinov, I. N. Mishustin, J. P. Bondorf, R. Donangelo, and K. Sneppen, Nucl. Phys. **A475**, 663 (1987).

[18] Some of the approximations invoked in Ref. [17] are also found in Ref. [19]. Readers should therefore examine the papers in Ref. [9] rather than Ref. [19] for further details concerning the SMM approach adopted in this paper.

[19] J. P. Bondorf, A. S. Botvina, A. S. Iljinov, I. N. Mishustin, and K. Sneppen, Phys. Rep. **257**, 133 (1995).

[20] To be consistent with the thermodynamical expressions for the free energy, we handle the term involving the spin degeneracy factor $g_{AZ}^{\mathrm{g.s.}}$ differently than it is handled in Ref. [9]. Within the approximation in Ref. [9] of $g_{AZ}^{\mathrm{g.s.}}=1$, this term vanishes.

[21] K. Sneppen, Nucl. Phys. **A470**, 213 (1987).

[22] H. Xi, W. G. Lynch, M. B. Tsang, and W. A. Friedman, Phys. Rev. C **54**, 2163 (1996).

[23] J. P. Bondorf, A. S. Botvina, and I. N. Mishustin, Phys. Rev. C **58**, 27 (1998).

[24] H. Xi, W. G. Lynch, M. B. Tsang, W. A. Friedman, and M. Durand, Phys. Rev. C **59**, 1567 (1999).

[25] T. K. Nayak, T. Murakami, W. G. Lynch, K. Swartz, D. J. Fields, C. K. Gelbke, Y. D. Kim, J. Pochodzalla, M. B. Tsang, H. M. Xu, F. Zhu, and K. Kwiatkowski, Phys. Rev. C **45**, 132 (1992).

[26] W. Hauser and H. Feshbach, Phys. Rev. **87**, 366 (1952).

[27] U. Lynen, R. Bassini, M. Begemann-Blaich, Th. Blaich, H. Emling, A. Ferrero, S. Fritz, S. J. Gaff, C. Groß, G. Immé, I. Iori, U. Kleinevoß, G. J. Kunde, W. D. Kunze, V. Lindenstruth, M. Mahi, A. Moroni, T. Möhlenkamp, W. F. J. Müller,

B. Ocker, T. Odeh, J. Pochodzalla, G. Raciti, Th. Rubehn, H. Sann, M. Schnittker, A. Schüttauf, C. Schwarz, W. Seidel, V. Serfling, J. Stroth, W. Trautmann, A. Trzcinski, G. Verde, A. Wörner, H. Xi, E. Zude, and B. Zwieglinski, Nucl. Phys. **A630**, 176 (1998).

[28] J. Pan and S. Das Gupta, Phys. Lett. B **344**, 29 (1995).

[29] William A. Friedman, Phys. Rev. C **42**, 667 (1990).

[30] N. Marie, A. Chbihi, J. B. Natowitz, A. Le Fèvre, S. Salou, J. P. Wieleczko, L. Gingras, M. Assenard, G. Auger, Ch. O. Bacri, F. Bocage, B. Borderie, R. Bougault, R. Brou, P. Buchet, J. L. Charvet, J. Cibor, J. Colin, D. Cussol, R. Dayras, A. Demeyer, D. Doré, D. Durand, P. Eudes, J. D. Frankland, E. Galichet, E. Genouin-Duhamel, E. Gerlic, M. Germain, D. Gourio, D. Guinet, K. Hagel, P. Lautesse, J. L. Laville, J. F. Lecolley, T. Lefort, R. Legrain, N. Le Neindre, O. Lopez, M. Louvel, Z. Majka, A. M. Maskay, L. Nalpas, A. D. Nguyen, M. Parlog, J. Péter, E. Plagnol, A. Rahmani, T. Reposeur, M. F. Rivet, E. Rosato, F. Saint-Laurent, J. C. Steckmeyer, M. Stern, G. Tabacaru, B. Tamain, O. Tirel, E. Vient, C. Volant, and R. Wada, Phys. Rev. C **58**, 256 (1998).